Brake Caliper Design and Optimisation for a Formula Student Vehicle

Diogo Paulo Martins Ferreira
diogopmferreira@tecnico.ulisboa.pt

Instituto Superior Técnico, Lisboa, Portugal

November 2019

Abstract

Finding the best suitable solution for each component of the car has been the objective of many formula student teams, similarly to the professional motorsport industry. This research is focused on the car's brake caliper replacement by an additive manufactured solution. The current system was analysed, resulting in a 10000 Nmm compliance objective for the new design. The new piston diameter was specified as 25mm. The topology optimisation results interpretation ended in a 12.5% lighter caliper. A transient heat transfer model has shown a settling temperature of 480°C after two circuit laps, bearable for both the caliper and discs. The manufacturing of the caliper was introduced with the necessary changes to be made on the caliper to allow the later post-processing machining with tolerance dimensions. An alternative solution was proposed, created with facets editing capable software, resulting in a most accurate topology recreation and in a 23% lighter component. The conclusions between the three components were made, focusing on compliance maintenance, percentage of weight reduction and cost comparison from the production point of view. The final solution production cost is around 550€, while the current solution selling price is 634€.

Keywords: Calipers, Additive manufacturing, Formula Student, Topology optimisation, Mechanical design, Selective Laser Melting

1. Introduction

Additive manufacturing technologies, after 30 years of development are now getting along within almost all production sectors, allowing the decrease of manufacturing steps over a determined part, reducing the waste of time and material.

The formula student competition is a source of innovation, where new designs can make the difference in the outcome result. The teams are influenced to test new solutions every year to keep up with the competition level. With this type of mindset, searching simultaneously for innovation and performance can be only achieved if the basic principles of vehicle performance are taken into consideration, such as the case of acceleration and deceleration. If these two characteristics become perfectly tuned, the car can get the most out of the track, since there is less time wasted on performing a brake to a corner or even reaching the top speed on a straight piece of track. To achieve those goals, the brake design can be optimised to increase the ratio performance/weight when compared to standard automotive road brakes.

The link between the brake system and an additive manufacturing implementation is the avoidance of unnecessary body shapes constrained by the manufacturing techniques, allowing the achievement of a topologically optimised body, capable of handling the necessary loads and temperatures, while being simultaneously lightweight.

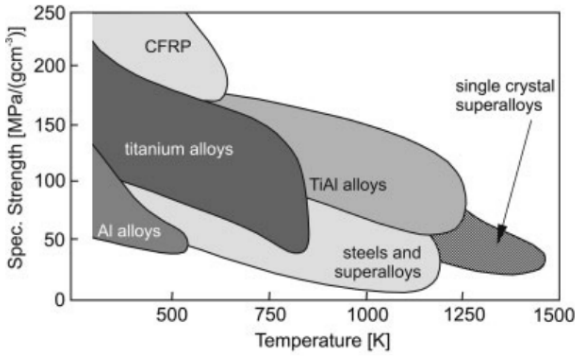

Figure 1: Specific Strength of the commonly used materials against temperature [1]

State of the art solutions in 3D printing are now exploring the versatility of the Ti6Al4V alloy, also called Titanium grade 5. There are several variants of titanium alloys, all of them with excellent

properties. However, this alloy is known for its key features, such as the weldability, high-temperature resistance of up to 800°, the biocompatibility and the high strength-to-weight ratio (Figure 1) [2]. It is an exceptional material with performance levels closer to the carbon fibre reinforced polymers and some extra commodities of the metal field.

2. Background

2.1. Competition Rules

Due to the nature of the competition and being the prototypes entirely made by students, there is a set of rules to be strictly met while building the car. Therefore, there are some of them strictly made to affect the design process of the brake system, fulfilling all the security procedures related to minimum brake performance.

The most important rules to be considered are [3]:

- The brake system must be capable of locking all four wheels at the same time;
- The vehicle must be equipped with a hydraulic brake system acting on all wheels and operated by one single control/pedal.
- The brake pedal and all the system must be designed to withstand a force of 2 kN without the failure of any component.
- The brake system must have two independent hydraulic lines such that in the case of leak or failure, there is still braking power to be applied in, at least, two of the wheels.

2.2. Relevant Car Specifications

The car specifications are critical to defining some reference values that play an important role in the design stage. Being this about the design of a brake system, the most important specifications to take into account are:

- Weight and Centre of Gravity position
- Aerodynamic forces Centre of Pressure position
- Wheel base
- Pedal Ratio
- Tire Radius
- Brake disc Effective Radius

2.3. Friction Model - Coulomb model

There is a simple model that can be used to securely design a brake system, being the static friction Coulomb model. Coulomb has determined that the frictional force produced by the contact between to bodies depends if the bodies are in static or kinetic contact.

The friction force, F_s, depends on the contact normal force, F_N, by the following equation:

$$F_s = \mu_s F_N \tag{1}$$

The μ_s is called the static friction coefficient, being dependent on the material but independent of the contact area [4].

For the kinetic friction, the kinetic friction force, F_k is dependent on the reasonable force of contact F_N, and it is not dependent on the sliding speed. The equation is kept same except for the μ_s, being replaced by the kinetic friction coefficient, μ_k [4].

$$F_k = \mu_k F_N \tag{2}$$

The meaning of these coefficients is related to the difference between the apparent area of contact and the real area of contact, noticeable at a micro-scale analysis of the contact surfaces. For a wide range of magnitudes of the normal force, it can be considered that the material is usually stiff enough to maintain a reasonable difference between the two areas referred to earlier.

2.4. Additive Manufacturing (AM)

AM technologies are defined as processes based on material addition instead of the common subtractive machining techniques. It is present for the last 25 years, being early restricted to polymer materials, making most of the parts produced not suitable for heavy-duty engineering purposes.

With this technology development, today, it is possible to see AM technologies incorporated in production and assembly lines of several industry fields [5]. The major benefits are those listed below:

- No tooling needed.
- Small production batches are economical - Setups are versatile.
- Reduced waste.
- Easy design changes and customization.

Table 1 shows the currently available techniques used by the additive manufacturing field. In the metal 3D printing, the commonly used technologies are laser melting techniques, that use metal powders as raw material.

The most relevant processes for this work are the SLS (*Selective Laser Sintering*) or SLM (*Selective Laser Melting*).

The SLS process heats the powder to a specific point where the material grains start the fuse together. Enough to create a solid and robust piece with the loose powder being cleaned up and removed later [6].

The SLM process, which can also be called DMLS (*Direct Metal Laser Sintering*), is very similar, but

Table 1: Additive manufacturing processes and suitable materials [5].

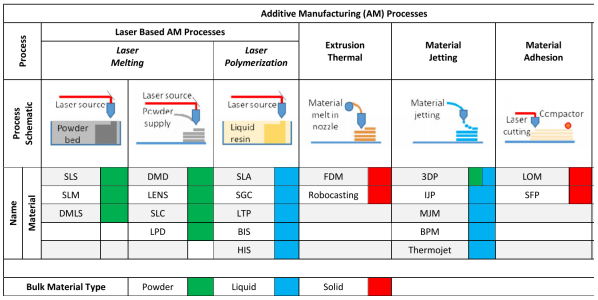

the powder is fully melted so that the material binds in the liquid state. It allows better control of the part porosity and structural integrity, but also requires more support structures to prevent the warping due to high residual stresses. These residual stresses are relieved after the heat treatment of the part, which guarantees better properties of the material [6].

3. Mechanical Analysis

3.1. Free Body Diagram Analysis

Once the driver hits the brakes, the tire's rolling resistance suddenly increases and therefore the friction force on the contact patch also increases. The sum of the friction forces acting on the four contact patches generates the deceleration force.

There is also another critical phenomenon called mass transfer that occurs because the CG of the car is not at the same height comparing to the contact patches, where the brake force acts. This phenomenon is responsible for changing the weight distribution through the tires, and consequently, modifying their braking behaviour, since the maximum static friction force suffers changes. Once the brake torque applied overcomes the torque caused contact patch friction, the wheels lock and the friction force suffers a reduction which cause a brake capacity loss. In order to obtain the critical loads for each tire, it has to be obtained first the maximum theoretical deceleration, d_M, that the car can achieve.

$$F_{smax} = \mu_s W_c = \sum_{i=1}^{4} F_{s_i} \tag{3}$$

$$F_{smax} = \frac{W_c}{g} d_M \Leftrightarrow d_M = \mu_s \, g \tag{4}$$

where F_{smax} is the maximum total friction force, F_{s_i} are the friction forces of each wheel and W_c is the car weight. To express the maximum deceleration in $g's$, g_M, then:

$$g_M = \mu_s \tag{5}$$

3.2. Free Body Diagram with Aerodynamic Influence

$$F_{smax} = \mu_s (W_c + F_A) \tag{6}$$

$$F_{smax} = \frac{W_c}{g} d_M \Leftrightarrow d_M = \frac{\mu_s \, g}{W_c} (W_c + F_A) \tag{7}$$

where F_A is the aerodynamic downforce. To express the maximum deceleration in $g's$, then:

$$g_M = \frac{\mu_s}{W_c} (W_c + F_A) \tag{8}$$

3.3. Forces Calculation

Based on the maximum deceleration, g_M, calculated earlier, it is possible to estimate all the essential values necessary to the system design.

Table 2: FST 09e car's specifications

Specs.	Value
Car Weight with driver, W_c	$300\,kg = 2943N$
CG Height, Y_{CG}	$0.3\,m$
Tire Radius, R	$0.22987\,m$
Tire Pressure, P_{tire}	$14.5\,psi = 99973.97\,Pa$
Tire Friction Coefficient, μ_{tire}	1.8
Wheelbase, L	$1530\,mm$
Pad Friction Coefficient, μ_{pad}	0.56
Mean Brake Disc Radius, r_m	$83\,mm$
Top Speed, u_{max}	$105\,km/h = 29.2\,m/s$
Coefficient of Lift, C_L	2.45
Frontal Projected Area, A_{proj}	$1.182\,m^2$
CG Longitudinal Position (driver included), x_{CG}	$48\%Front\ 52\%Rear$
CP Longitudinal Position, x_{CP}	$45\%Front\ 55\%Rear$
Brake Pedal Ratio, PR	3.53
MC Bore Diameter	$15\,mm$

$$C_L = \frac{2F_A}{\rho_{air} u^2 A_{proj}} \Leftrightarrow F_A \approx 1481N \tag{9}$$

$$g_M = \frac{1.8}{2943}(2943 + 1481) = 2.7 g's$$

$$Fv_f = 0.48 W_c + 0.45 F_A = 2079N$$

where ρ_{air} is the air density, u^2 is the square velocity and A_{proj} is the aerodynamic frontal projected area. It is now determined the total front axle vertical force, F_f, as the sum of the static vertical force, Fv_f with the mass transfer force, F_{mt}.

$$F_f = Fv_f + F_{mt} \tag{10}$$

$$F_{mt} = \frac{F_{inertia} Y_{CG}}{L} \tag{11}$$

$$F_f = 2079N + \frac{W_c \; g_M Y_{CG}}{L} \approx 3640N$$

$$F_{fwheel} = F_f / 2 = 1820N$$

The F_{fwheel} is the vertical load on each front wheel, being basically the half split of F_f. Knowing the total wheel load, it can be calculated the maximum Brake Force, F_{brake} and then the maximum Brake Torque, T_{brake}. To calculate the torque, it is necessary to determine the real tire radius, represented in figure 2.

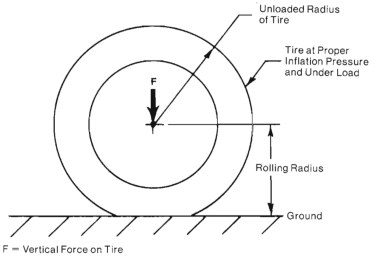

Figure 2: Real rolling radius due to tire load and pressure [7]

$$F_{brake} = \mu_{tire} F_{fwheel} \tag{12}$$

$$F_{brake} = 1.8 \times 1820 = 3276N$$

$$T_{brake} = F_{brake}\, R_{loaded} \tag{13}$$

$$R_{loaded} = \sqrt{(\frac{-F_{fwheel}}{2P_{tire}\, l})^2 + R^2} \tag{14}$$

$$R_{loaded} = 0.224m$$

$$T_{brake} = 734.2Nm$$

So for a chosen driver's foot force of $600N$ to achieve the maximum deceleration, the next step is determining how much enhancement does that force suffers due to the pedal ratio.

$$F_{balancebar} = F_{pedal}\, PR \tag{15}$$

$$F_{balancebar} = 600 \times 3.53 = 2121.9N$$

The brake bias is the split ratio of the $F_{balancebar}$ amongst the MC. The balance bar mechanism is explained in figure 3. Adjusting the brake

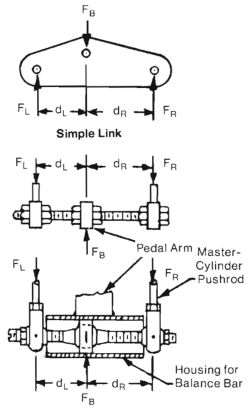

$$F_R{}^1 = F_B \frac{d_L}{d_L + d_R} \tag{16}$$

$$F_L{}^2 = F_B \frac{d_R}{d_L + d_R} \tag{17}$$

$$F_B{}^3 = F_L + F_R \tag{18}$$

Figure 3: Balance Bar setup [7]

bias to 70% at the front and 30% at the rear, the force on the front MC is $1485.3N$. This adjustment decreases the rear brake line pressure, which may not be used due to smaller brake capabilities of the rear tires. The front line pressure, $P_{frontline}$ can be obtained by:

$$P_{frontline} = \frac{F_{frontMC}}{\pi r^2} \tag{19}$$

$$P_{frontline} = 8.405\, MPa$$

Now, as it is defined that there are four pistons on the front caliper, to assure a smoother and even friction on the pads, it is possible to determine its diameter.

$$A_{fpiston} = \frac{T_{brake}}{2 \times 2 \times \mu_{pad} \times \mu_{disc} \times P_{frontline} \times r_m} \tag{20}$$

$$D_{fpiston} = \sqrt{\frac{4A_{fpiston}}{\pi}} \tag{21}$$

where the r_m is the disc mean radius, $A_{fpiston}$ is the piston contact area and μ_{disc} is an efficiency factor used for disc brake systems that is usually 0.96. The result is a $D_{fpiston}$ equal to $25mm$.

4. Design

4.1. Design Process

The final result for the base model was a part where a non-design space had to be defined in order to keep the minimum necessary characteristics while optimising topologically, shown in figure 4.

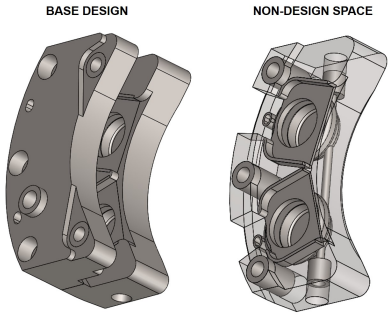

Figure 4: Base design and optimisation spaces definition

4.2. Optimisation Model Setup

4.2.1 Topology Optimisation Formulation

For a structural problem like this the design variable is the element relative density, ρ_e, that defines basically the existence of the absence of that element. The problem formulation is stated below in the system 22.

$$\begin{cases} \min & f(\tilde{\rho}, \mathbf{u}(\tilde{\rho})) \\ \text{subjected to} & \begin{cases} \text{equilibrium equation} \\ \text{design constraints} \\ \text{manuf. contraints} \end{cases} \end{cases} \tag{22}$$

[1] Right MC force (figure 3)
[2] Left MC force (figure 3)
[3] Balance bar force (figure 3)

The function f is the objective function of the problem, that in this case will be the volume of the structure. The volume is given by the the internal product between the elementary volume vector and the elementary density vector.

$$\min\ f = \min\ \tilde{V}_e.\tilde{\rho} \tag{23}$$

The vector $\mathbf{u}$ is the displacement vector of the mesh nodes that is dependent of the $\tilde{\rho}$ vector, which contains all the element relative densities. The equilibrium equation is given by:

$$\mathbf{K}(\tilde{\rho})\,\mathbf{u}(\tilde{\rho}) = \mathbf{F} \tag{24}$$

where $\mathbf{K}$ is the stiffness matrix of the problem and $\mathbf{F}$ is the global load vector.

To evaluate the effect of intermediate densities in the structural integrity of the model, there is an interpolation of the element stiffness, according to figure 5 and equation 25. The p is the penalty factor and those curves are the SIMP method curves, whose method is described by equation 25. For the same density, the relative stiffness of the element gets lower with the increase of the penalty factor. The penalised formulation leads the element densities to values closer to 1 or 0, i.e. the material presence or absence. The design and non-design space are defined through this variable.

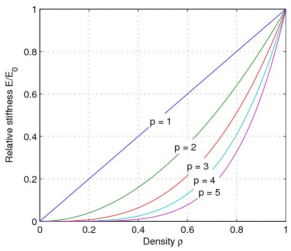

$$\mathbf{E} = \mathbf{E^0}\,{\rho_e}^p \tag{25}$$
$$\rho_e \in [0,1], \quad p \geq 1$$

Figure 5: SIMP method curves with different penalty factors [8]

$$\rho_e = \begin{cases} 1, & \text{if } e \in \text{non-design space} \\ [0,1], & \text{if } e \in \text{design space} \end{cases} \tag{26}$$

To assure the proper stiffness, there is a compliance constraint obtained from a car's current brake system analysis. The result was $10^4\,Nmm$ and compliance is defined by equation 27.

$$\mathbf{C} = \mathbf{F}^T\,\mathbf{u}(\tilde{\rho}) \tag{27}$$

4.2.2 Model Description

There are three loads present on the model, such as the line pressure, the brake torque and the bolts pretension.

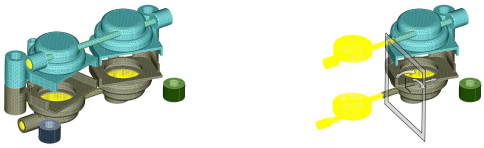

Figure 6: Line pressure represented on FEM model

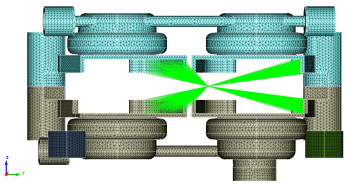

Figure 7: Brake torque represented on FEM model

Figure 8: Bolt pretension represented on FEM model

Table 3: Ti6Al4V material properties

Properties	Value
E-Modulus	104-124 GPa
Yield strength, S_y	min. 860 MPa
Ultimate Tensile strength, S_{ut}	min. 930 MPa
Density, ρ	4.41 g/cm^3
Air and Watertight	yes
Max. Operating Temperature	350°C

Using a safety factor of 1.5 and the minimum properties values, the maximum allowable stress is $570MPa$. The brakes are a safety system therefore they were designed for infinite life in terms of fatigue. According to [9], the Ti6Al4V alloy fatigue strength, S_e, for high cycle fatigue behaviour, is $507\,MPa$.

With the modified Goodman line, the load problem is transformed to a fully reversible load case, resulting in $\sigma_{max} \approx 440\,MPa$, being the maximum stress constraint imposed. The optimisation problem is summed to the following system:

$$\begin{cases} \min & \tilde{V}_e.\tilde{\rho} \\ \text{subjected to} & \begin{cases} \mathbf{Ku} = \mathbf{F} \\ \mathbf{C} - 10^4 \leq 0 \\ \sigma_{vm} - 440 \leq 0 \end{cases} \end{cases}$$

4.3. First Result

The optimisation result plot shows the elements densities between 0 and 1. A threshold value must

be used as a result to define the final result, being the minimum density value showed in the plot. The used value was 0.3 because it showed a good continuity between the different design spaces.

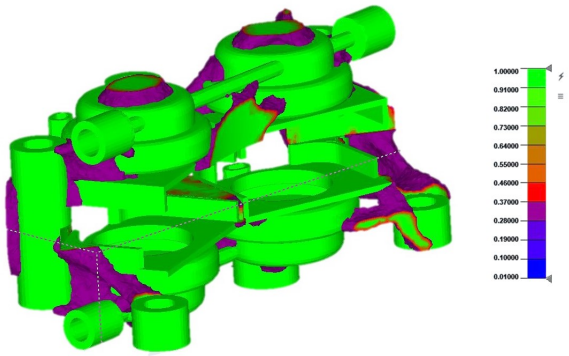

Figure 9: 0.3 threshold

Table 4: First solution

Properties	Value
Compliance	5674
Weight (Caliper+Pistons)	$350g$
Maximum Displacement	$0.69mm$

Figure 10: First result render

5. Thermal Analysis

5.1. Theoretical Model

The thermal effusivity, α, is a measure for the capability of a material to exchange thermal energy with its surroundings.

$$\alpha = \sqrt{k\rho c} \tag{28}$$

being k, ρ and c the thermal conductivity, material density and specific heat capacity, respectively, whose values are represented in table 5. A theoretical model to determine the heat distribution between the dics and pads [10], is given by:

$$p_D = \frac{\alpha_D A_D}{\alpha_D A_D + \alpha_P A_P} \tag{29}$$

$$p_P = 1 - p_D \tag{30}$$

where p_D is the brake disc heat dissipation ratio and p_P is the brake pads heat dissipation ratio.

Table 5: Friction couple properties

Specs.	Disc	Pad
Density, ρ	$7860\,kg/m^3$	$2600\,kg/m^3$
Thermal Conductivity, k	$50\,W/m\,K$	$12\,W/m\,K$
Specific heat capacity, c	$500\,J/kg\,K$	$1465 J/kg\,K$
Area of friction	$19512\,mm^2$	$3755\,mm^2$

5.2. Transient Heat Transfer Model Setup

The figures 11 and 12 show the heat fluxes application areas and the convection dissipation faces defined on the model. The equation 31 defines the forced convection coefficient that is velocity dependent, according to [11].

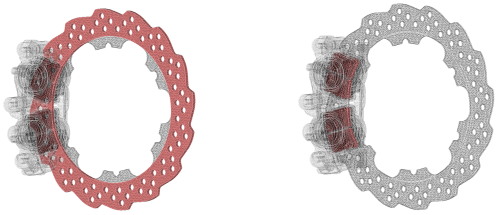

(a) Brake disc (b) Pad area

Figure 11: Defined areas for heat flux application

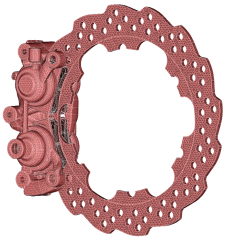

$$h_{forced} = 17v + h_{natural} \tag{31}$$

Figure 12: Convection relevant faces

The car was equipped with a camera capable of collection GPS and accelerometer data. Knowing the acceleration and velocity transient response, the braking power, $P_{braking}$, can be calculated by:

$$F_{braking} = m \times a \tag{32}$$

$$P_{braking} = F_{braking} \times v \tag{33}$$

Using the brake bias, BB, defined before, the disc and pads dissipated power is calculated by:

$$P_{disc} = \frac{P_{braking} \times BB \times p_D}{2} \tag{34}$$

$$P_{pads} = \frac{P_{braking} \times BB \times p_P}{2} \tag{35}$$

The disc and pads heat fluxes are obtained with:

$$\Psi_{disc} = \frac{P_{disc}}{A_{disc}} \tag{36}$$

$$\Psi_{pads} = \frac{P_{pads}}{A_{pads}} \tag{37}$$

5.3. Transient Heat Transfer Model with Aerodynamics and Brake Regeneration

The drag force, F_{aero}, and the aerodynamic dissipation power, P_{aero} is defined by:

$$F_{aero} = \frac{C_D \times v^2 \times \rho_{air} \times A_{proj}}{2} \tag{38}$$

$$P_{aero} = F_{aero} \times v \tag{39}$$

The brake regeneration capabilities of the car are capped at $15kW$ and can be either enabled or disabled.

$$P_b = \begin{cases} P_{regen} & \text{if } P_b \in [0, 15] \\ P_{regen} + P_{aero} & \text{if } P_b \in [15, 15 + P_{aero}] \\ P_{aero} + P_{mec} + P_{regen} & \text{if bigger} \end{cases} \tag{40}$$

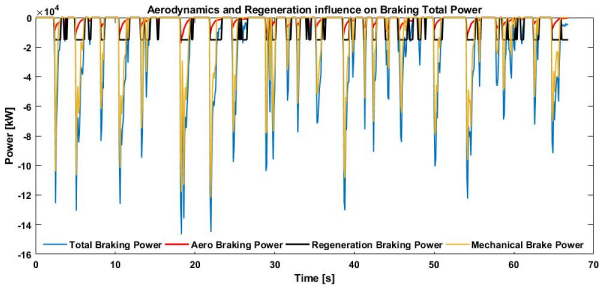

Figure 13: Aerodynamics and Regeneration In ence on Braking Total Power

5.4. Hub influence

The hub's inclusion as a dissipation medium implemented, but there is an operating tempe ture at specific faces of the hub. Those faces close or in direct contact with the transmission its lubricant, where heat is generated. Those fa were set to an operating temperature of $75°C$, cording to [12].

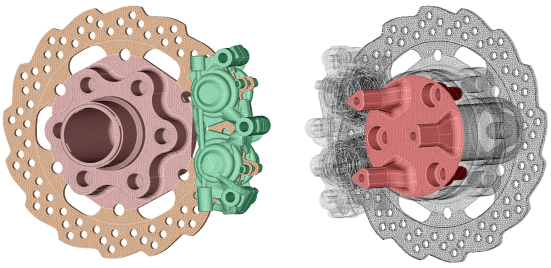

(a) Hub assembled (b) Faces at operating temperature

Figure 14: Second thermal model scheme

5.5. Results

These transient analysis represent an autocross lap at the Formula Student Spain competition.

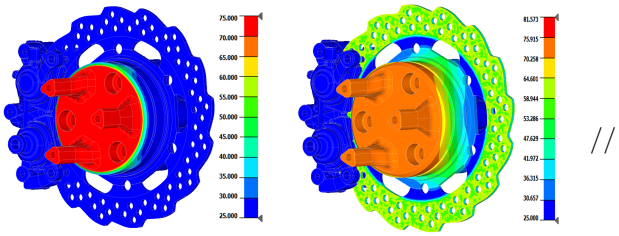

(a) 0s system temperature (b) 2.7s system temperature

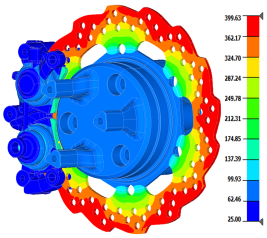

(c) 70s system temperature

Figure 15: Temperature plot at different stages of autocross - Model 2

To evaluate the stability of the system temperatures, a new analysis was performed considering two consecutive laps. The maximum temperature after consecutive runs is 485°C.

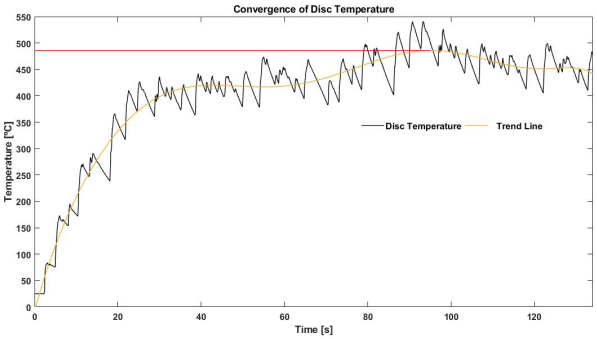

Figure 16: Convergence of Disc Temperature

6. Alternative Design

The strategy to obtain a different and possibly better solution was the use of facets editing software. The first solution is still way below the compliance limit, due to the conversion of intermediate densities elements in fully densed elements, but also due to the geometry simplification while replicating the topology optimisation result.

However, this alternative software makes it possible to use smoothing and wrapping algorithms to create a smooth and bonded connection, between the different design spaces

This new optimisation solution came with an additional constraint. It consists in a minimum size

dimension filter of 5mm, to reduce small sized features, that have higher tendency to warp.

6.1. Alternative Design Result

Figure 17 shows the new topology design for the same density threshold, while table 6 shows its properties.

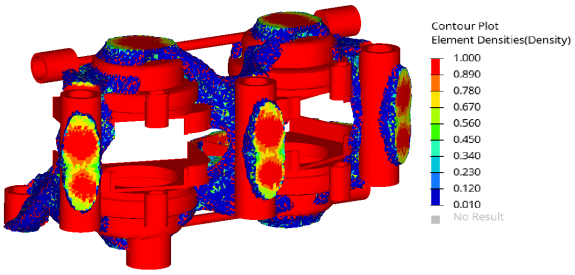

Figure 17: Alternative design isosurface

Table 6: Alternative Solution

Properties	Value
Compliance	8633
Weight (Caliper+Pistons)	$308g$
Maximum Displacement	$0.82mm$

Figures 18 and 19 show the automatic design process through this method. To a better understanding of the final part appearance, figure 20 shows a rendered perspective view.

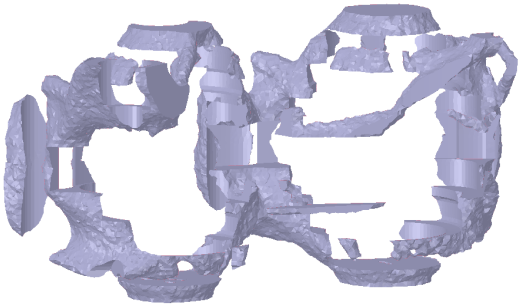

Figure 18: 0.3 density threshold isosurface

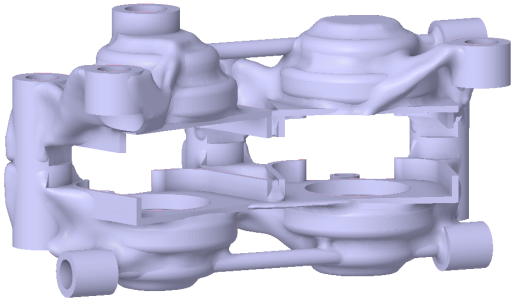

Figure 19: Final faceted part

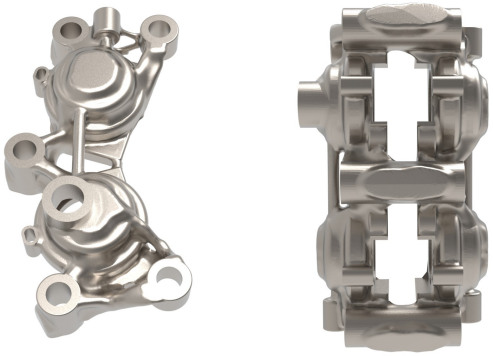

Figure 20: Faceted design render view

7. Conclusions

7.1. Detailed comparison between solutions

The current front caliper of the car is the AP Racing CP4227-2S0 (Figure 21). It is an aluminium racing caliper made especially for bikes but suitable for the car requirements, whose properties are specified on table 7

Figure 21: AP Racing Caliper

Table 7: AP Racing Solution

Properties	Value
Compliance	10000
Weight (Caliper+Pistons)	$400g$
Maximum Displacement	$0.82mm$

The major part of components are kept similar, therefore the conclusion analysis falls upon the caliper and the pistons, that are in this case, the only commutable components. The first solution presented a 12.5% mass reduction, while the alternative achieved a 23% mass reduction. However, the alternative design has reduced the compliance by 14%, which is a smaller compliance reduction compared to the first solution, but within the compliance limit, therefore more than acceptable.

The thermal analysis has served to corroborate the disc temperature and its maximum settling point during consecutive runs but also shown that the caliper temperature is within the bearable range for this type of titanium alloy.

To further evaluate the cost of the AM solution, it was used the Atzeni and Salmi economic study [13]. It must be clear that this cost analysis is from the production point of view. The following procedure was considered:

- The volume is 110% of the part volume to account for supports and wasted material that the 3D printer used at the building plate;
- It considers that each machine has around 5 years of linear depreciation to determine the hourly cost;
- It considers that the use percentage of the machine will around 60% per year when normally those machines can operate at the 80% range;
- It considers the SLM 280 machine from SLM Solutions with a price tag around 400 000€;
- The build plate size is $280 \times 280 \times 365mm$. Capable of manufacture two halves, i.e. one caliper.

A study to determine the optimal set of parameters for a high quality Ti6Al4V alloy SLM printing resulted in a build up time of $9.6h$ for this specific print [14].

The cost of each solution was analysed and compared with the market selling price of the AP Racing caliper. The cost analysis is detailed on the table 8.

Table 8: AM design cost analysis

Number of parts produced per job	-	N	1 (two halves)
Material cost per kg	EUR/kg	M	350
Mass of material per part	kg	U	0.385
Material cost per part	EUR	MP=U×M	135
Machine operator cost per hour	EUR/h	O	20
Set up time	h	A	1.2
Pre-processing cost per part	EUR	AP=A×O/N	24
Depreciation cost per year	EUR/year	C	80000
Hours per year	h/year	H=0.6×365*24	5256
Machine cost per hour	EUR/h	CH=C/H	15.2
Job time	h	T	9.6
Machine cost per job	EUR	CB=CH×T	34.96
Processing cost per part	EUR	CP=CB/N	67.5
Post-Processing time per job	h	B	1.5
Heat treatment cost per job	EUR	HT	20
Post-processing cost per part	EUR	BP=(O×B+HT)/N	50
Total cost per part	EUR	P=MP+AP+CP+BP	≈422

Some extra costs were not accounted at first, such as post processing machine cost per hour, consumables and maintenance, energy and the 3-axle CNC milling. Therefore, they were added later, resulting in 80€ extra per part for extra cost plus 48€ per part for the CNC milling, according to [15] [16].

The final results expected are a 550€ and 531€ price for the production of the first and alternative solution, respectively. The selling price of the AP Racing caliper is 634€.

Despite this cost being lower than the AP racing caliper, it has to be considered that the AP racing price is the selling price with the profit margin and taxes included on top of the manufacturing cost, while the table analysis is the cost from the production point of view. As a Formula Student team, this approach may be valid, since it is possible to negotiate the terms with some sponsors, that may not be able to sponsor printed parts fully, but may be able to accept a deal of production costs payment, leaving the profit margin and taxes at the side, in return of the visibility. There is also the possibility of splitting the cost between different sponsors if one is in charge of the material supply and the other in charge of the machinery work, for example.

In the typical industry point of view, this cost analysis will not be acceptable, unless the entity already has this piece of machinery. If the hardware is available, it is possible to produce those components at that price. Otherwise, the costs of ordering these 3D printed components may be estimated by asking for a quote to a known company. As an example, a quote asked to Sculpteo company estimates that the production of one caliper is 1952€. Depending on the batch size, the costs may reduce, but will always be much higher than the previous calculated.

References

[1] Manfred Peters and Christopher Leyens. *Titanium and Titanium Alloys*. Wiley, jul 2003.

[2] Titanium Processing Center. Titanium TI-6AL-4V Properties & Common Uses, 2016. `https://titaniumprocessingcenter.com/titanium-ti-6al-4v-properties-common-uses/`, Last acessed on 21/10/2019.

[3] FS-Germany. Formula Student Rules 2019 V1.1, 2019. `https://www.formulastudent.de/fileadmin/user_upload/all/2019/rules/FS-Rules_2019_V1.1.pdf`, Last acessed on 29/10/2019.

[4] Valentin L. Popov. *Contact Mechanics and Friction*. Springer Berlin Heidelberg, 2nd edition, 2017.

[5] R. Singh and S Singh. *Additive Manufacturing: An Overview*. Elsevier, 2017. `https://linkinghub.elsevier.com/retrieve/pii/B9780128035818041655`, Last acessed on 23/10/2019.

[6] Introduction to 3D Printing - Additive Processes. `https://make.3dexperience.3ds.com/processes/powder-bed-fusion` ,Last acessed on 23/10/2019.

[7] Fred Puhn. *Brake Handbook*. HP Books, 1985.

[8] Anton Olason. Methodology for Topology and Shape Optimization in the Design Process.

Master's thesis, Chalmers University of Technology, Sweden, 2010.

[9] M. Janeček, F. Nový, P. Harcuba, J. Stráský, L. Trško, M. Mhaede, and L. Wagner. The Very High Cycle Fatigue Behaviour of Ti-6Al-4V Alloy. *Acta Physica Polonica A*, 128(4):497–503, oct 2015.

[10] Adriaan Neys. In-Vehicle Brake System Temperature Model. Master's thesis, Chalmers University of Technology, Sweden, 2012.

[11] Manthan Vidiya and Balbir Singh. Experimental and Numerical Thermal Analysis of Formula Student Racing Car Disc Brake Design. *Journal of Engineering Science and Technology Review*, 10(1):138–147, feb 2017.

[12] Luís Miguel Marcos de Abrunhosa Vieira de Abreu. Mechanical design of the wheel assembly of an electric Formula Student prototype. Master's thesis, Instituto Superior Técnico, Portugal, May 2019.

[13] Eleonora Atzeni and Alessandro Salmi. Economics of additive manufacturing for end-usable metal parts. *The International Journal of Advanced Manufacturing Technology*, 62(9-12):1147–1155, oct 2012.

[14] Zhonghua Li, Ibrahim Kucukkoc, David Z. Zhang, and Fei Liu. Optimising the process parameters of selective laser melting for the fabrication of Ti6Al4V alloy. *Rapid Prototyping Journal*, 24(1):150–159, jan 2018.

[15] Zhengdong Liu. ECONOMIC COMPARISON OF SELECTIVE LASER MELTING AND CONVENTIONAL SUBTRACTIVE MANUFACTURING PROCESSES. Master's thesis, Northeastern University, Massachusetts, May 2017.

[16] FST Lisboa. Cost Explanation File (CEF). Technical report, 2019.